FRA-91-2

U.S. Department
of Transportation
**Federal Railroad
Administration**

Dynamic Buckling Test Analyses of a High Degree CWR Track

Office of Research and
Development
Washington, DC 20590

A. Kish
G. Samavedam

U.S. Department of Transportation
Research and Special Programs Administration
John A. Volpe
National Transportation Systems Center
Cambridge, MA 02142

DOT/FRA/ORD-90/13
DOT-VNTSC-FRA-91-2

February 1991
Final Report

NOTICE

This document is disseminated under the sponsorship of the Departments of Transportation and Defense in the interest of information exchange. The United States Government assumes no liability for its contents or use thereof.

NOTICE

The United States Government does not endorse products or manufacturers. Trade or manufacturers' names appear herein solely because they are considered essential to the object of this report

Technical Report Documentation Page

1. Report No.	2. Government Accession No.	3. Recipient's Catalog No.
DOT/FRA/ORD-90/13		

4. Title and Subtitle	5. Report Date
Dynamic Buckling Test Analyses of a High Degree CWR Track	February 1991
	6. Performing Organization Code: DTS-76
7. Author(s): A. Kish, G. Samavedam*	8. Performing Organization Report No.: DOT-VNTSC-FRA-91-2
9. Performing Organization Name and Address: U.S. Department of Transportation, Research and Special Programs Administration, John A. Volpe National Transportation Systems Center, Cambridge, MA 02142	10. Work Unit No. (TRAIS): RR119/R1006
	11. Contract or Grant No.
12. Sponsoring Agency Name and Address: U.S. Department of Transportation, Federal Railroad Administration, Office of Research and Development, Washington, DC 20590	13. Type of Report and Period Covered: Final Report, September 1987-August 1990
	14. Sponsoring Agency Code: RDV-31

15. Supplementary Notes
*Foster-Miller, Inc.
350 Second Avenue
Waltham, MA 02254

16. Abstract

Thermal buckling of railroad tracks in the lateral plane is an important problem in the design and maintenance of continuous welded rail (CWR) tracks. The work reported here is part of a major investigation carried out by the John A. Volpe National Transportation Systems Center for the Federal Railroad Administration on the thermal buckling of CWR tracks with the objective of developing guidelines and recommendations for buckling prevention.

This report presents the results of two major buckling tests conducted on 7.5 degree curved CWR track at the Transportation Test Center, Pueblo, CO. In the first test, thermal buckling was induced in the absence of vehicles to evaluate the static buckling strength of the 7.5 degree curve with 1.5 in. line defect. In the second test, the dynamic buckling behavior of the curve (with typical line defects as in the revenue tracks) under vehicular traffic was studied. The buckling strength of the track under vehicle loads was determined in this test.

The test results, the analytical predictions, and conclusions of practical interest are presented in this report.

17. Key Words	18. Distribution Statement
Track Buckling, Dynamic Buckling, Lateral Stability, Continuous Welded Rails, High Degree Curve	DOCUMENT IS AVAILABLE TO THE PUBLIC THROUGH THE NATIONAL TECHNICAL INFORMATION SERVICE, SPRINGFIELD, VIRGINIA 22161

19. Security Classif. (of this report)	20. Security Classif. (of this page)	21. No. of Pages	22. Price
Unclassified	Unclassified	42	

PREFACE

The work in this report was sponsored by the United States Department of Transportation (DOT), Federal Railroad Administration (FRA), Office of Research and Development, Washington, DC.

The report presents the results of buckling tests on 7.5 degree curved continuous welded rail (CWR) track, conducted in the fall of 1987 at the Transportation Test Center, Pueblo, CO. The work presents a part of the John A. Volpe National Transportation Systems Center's (VNTSC) track stability research program being conducted for the FRA for the purpose of developing guidelines and specifications for the prevention of track buckling induced derailments.

The tests were conducted jointly by the Association of American Railroads (AAR) with the AAR at the Transportation Test Center (TTC), and Foster-Miller, Inc. under contracts with the U.S. DOT.

Thanks are due to W.R. Paxton of the FRA for his support throughout the various phases of the test program, and to Mr. M. Thurston of the VNTSC for data reduction and analysis.

Thanks are also due to Mr. D. Read of TTC for his participation and test support, and to Messrs. E. Dickinson and M. Nemirow of Foster-Miller, and Mr. R. Nicholay of TTC for design and operation of locomotive conversion and rail heating during the tests.

METRIC CONVERSION FACTORS

Approximate Conversions to Metric Measures

Symbol	When You Know	Multiply by	To Find	Symbol
		LENGTH		
in	inches	*2.5	centimeters	cm
ft	feet	30	centimeters	cm
yd	yards	0.9	meters	m
mi	miles	1.5	kilometers	km
		AREA		
in^2	square inches	6.5	square centimeters	cm^2
ft^2	square feet	0.09	square meters	m^2
yd^2	square yards	0.8	square meters	m^2
mi^2	square miles	2.6	square kilometers	km^2
	acres	0.4	hectares	ha
		MASS (weight)		
oz	ounces	28	grams	g
lb	pounds	0.45	kilograms	kg
	short tons (2000 lb)	0.9	tonnes	t
		VOLUME		
tsp	teaspoons	5	milliliters	ml
Tbsp	tablespoons	15	milliliters	ml
fl oz	fluid ounces	30	milliliters	ml
c	cups	0.24	liters	l
pt	pints	0.47	liters	l
qt	quarts	0.95	liters	l
gal	gallons	3.8	liters	l
ft^3	cubic feet	0.03	cubic meters	m^3
yd^3	cubic yards	0.76	cubic meters	m^3
		TEMPERATURE (exact)		
°F	Fahrenheit temperature	5/9 (after subtracting 32)	Celsius temperature	°C

*1 in = 2.54 (exactly). For other exact Conversions and more detailed tables, see NBS Misc. Publ. 286, Units of Weights and Measures, Price $2.25, SD Catalog No. C13.10:286.

Approximate Conversions from Metric Measures

Symbol	When You Know	Multiply by	To Find	Symbol
		LENGTH		
mm	millimeters	0.04	inches	in
cm	centimeters	0.4	inches	in
m	meters	3.3	feet	ft
m	meters	1.1	yards	yd
km	kilometers	0.6	miles	mi
		AREA		
cm^2	square centimeters	0.16	square inches	in^2
m^2	square meters	1.2	square yards	yd^2
km^2	square kilometers	0.4	square miles	mi^2
ha	hectares (10,000 m^2)	2.5	acres	
		MASS (weight)		
g	grams	0.035	ounces	oz
kg	kilograms	2.2	pounds	lb
t	tonnes (1000 kg)	1.1	short tons	
		VOLUME		
ml	milliliters	0.03	fluid ounces	fl oz
l	liters	2.1	pints	pt
l	liters	1.06	quarts	qt
l	liters	0.26	gallons	gal
m^3	cubic meters	35	cubic feet	ft^3
m^3	cubic meters	1.3	cubic yards	yd^3
		TEMPERATURE (exact)		
°C	Celsius temperature	9/5 (then add 32)	Fahrenheit temperature	°F

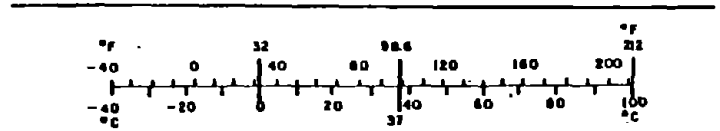

CONTENTS

LIST OF ILLUSTRATIONS

EXECUTIVE SUMMARY

The John A. Volpe National Transportation Systems Center (VNTSC) has been conducting experimental and analytic investigations on the buckling safety of continuous welded rail (CWR) tracks to support the safety mission of the Federal Railroad Administration (FRA). This report describes a part of these investigations related to the static and dynamic buckling behavior of a high degree curve (7.5 degree) CWR track.

The specific objectives of the work are:

a. To determine the static buckling strength of the 7.5 degree curve and correlate it with the theoretical predictions ;

b. To determine the dynamic buckling behavior of the high degree CWR curved track subjected to thermal and vehicle-induced loads ; and

c. To determine the "ultimate" dynamic buckling strength of the high degree CWR track at the maximum allowable speed.

To realize the foregoing objectives, tests were conducted at the Transportation Test Center (TTC), Pueblo, CO in September-October, 1987. The rail heating was provided by electric current drawn from alternators of two GP-32-2 locomotives. The test tracks were instrumented to determine the rail longitudinal forces, L/V (lateral to vertical wheel loads) ratio, lateral and longitudinal displacements and the rail temperature. For the dynamic buckling test, a consist of one locomotive and 24 loaded hopper cars, operating at 34 mph, was used.

The following conclusions are drawn:

a. The "dynamic buckling strength" of 7.5 degree curve with a lateral resistance of 1,780 lb./tie and with a line defect of 0.75 in. was found to be on the order of 62°F above the neutral temperature. The static buckling strength of a weaker track (lateral resistance 1,350 lb./tie and a line defect of 1.5 in.) is slightly higher (66°F above the neutral).

b. With increase in the rail temperature above the lower dynamic buckling temperature, the vehicles generated rapid growth of lateral misalignment. The allowable temperature for safe operations therefore should not be greatly different from this temperature.

c. The uplift bending wave seems to be primarily responsible to cause the maximum growth in the lateral misalignment by reducing the lateral resistance locally at the central region under vehicles. This is in accordance with the dynamic theory of buckling.

d. The progressive buckling behavior (rapid growth of misalignments under the test train) observed in this test suggests the need for additional high degree CWR curve studies for a more complete evaluation and quantification of buckling safety.

LIST OF SYMBOLS AND ABBREVIATIONS

P	Rail force in buckled zone
θ	Angular coordinate for curved track
R	Curve radius
$2L$	Buckling length
$2L_o$	Initial imperfection length
E	Modulus of rail steel
A	Cross sectional area (two rails)
I	Moment of inertia (two rails)
k_f	Longitudinal stiffness
F	Lateral resistance
F_p	Peak value of F
F_L	Limiting value of F
u	Longitudinal displacement in adjoining zone
U	Longitudinal displacement in buckled zone
w	Radial (lateral) displacement
w_o	Initial imperfection
$\dot{w}$, $\ddot{w}$	Primes denote derivatives
α	Coefficient of thermal expansion
T	Temperature rise
T_S	Lower buckling temperature increase
T_N	Neutral or stress-free temperature of rail

1. INTRODUCTION

The Federal Railroad Administration (FRA) sponsors the John A. Volpe National Transportation Systems Center's (VNTSC) research and development of safety specifications and guidelines for buckling prevention of continuous welded rail (CWR) track. A major element of this program is the investigation of CWR track stability under the influence of high thermal forces and vehicle induced loads. Under this program, dynamic buckling tests were planned by VNTSC and conducted by the Association of American Railroads/Transportation Test Center (AAR/TTC) at the TTC facility in 1983 (Phase I), 1984 (Phase II), 1986 (Phase III) and 1987 (Phase IV). The tests in Phases I, II, and III were performed on tangent and 5 degree curved tracks, and resulted in preliminary validation studies of buckling analyses and safety criteria presented in References (1,2). The Phase IV tests were conducted on a 7.5 degree curved CWR track. The purpose of this report is to present Phase IV test results and provide comparisons with analytic predictions.

In Phase IV, two major tests were conducted on a 7.5 degree curve. These consisted of a "static" buckling test and a dynamic buckling test. A major objective in Phase IV was to determine the ultimate dynamic buckling strength of the CWR curve for the purpose of verifying buckling safety limits currently under development by VNTSC.

The test track was 1,000-ft. long with soft wood ties with cut spike construction. Every tie had channel type rail anchors. The track was laid with 136-lb. CWR and had a 4.5-in. superelevation. The curvature was 7.5 degrees and the test zone had a grade of 1 percent. The ballast was AREA-4 slag with 12 to 16-in. shoulder width and full cribs.

Both the static and dynamic buckling tests were carried out until the track buckled out. For the dynamic buckling test, a consist of one locomotive and 23 loaded hopper cars and an empty hopper car operating at 34 mph was used. In the dynamic buckling test, both "progressive" and "explosive" types of buckling occurred at different locations in the test zone.

The test results and comparisons with the theories (3,4) are presented in this report.

2. THEORETICAL CONSIDERATIONS

The analytical predictions are performed using the buckling theory developed in References (3-5). In the theoretical formulation, the track is divided into a buckled zone in the region $|\theta| \leq \phi$, which experiences large lateral (radial) displacements and adjoining zones, $|\theta| \geq \phi$, which undergo essentially longitudinal (tangential) displacements (Figure 1). The relevant equilibrium equations are:

Buckled Zone $|\theta| \leq \phi$

$$\frac{EI}{R^4}\ddot{w} + \frac{\bar{P}w}{R^2} = -F(w) + \frac{\bar{P}}{R} + \frac{\bar{P}w_o}{R^2} \quad \text{(lateral equilibrium)} \qquad (1)$$

$$\frac{\dot{u}}{R} = -\frac{\bar{P}}{EA} - \frac{w}{R} + \frac{\dot{w}^2}{2R^2} + \frac{\dot{w}\dot{w}_o}{R^2} + \alpha T \quad \text{(longitudinal equilibrium)} \qquad (2)$$

The dots denote derivatives with respect to θ and P = compressive force in buckled zone, w = radial displacement, w_o = initial misalignment.

Adjoining Zones $|\theta| \geq \phi$

$$AE\ddot{u} = k_f u \quad \text{(longitudinal equilibrium)} \qquad (3)$$

where k_f is the track longitudinal stiffness

The radial equilibrium equation in the adjoining zones will be ignored since the radial displacements in these zones are expected to be very small.

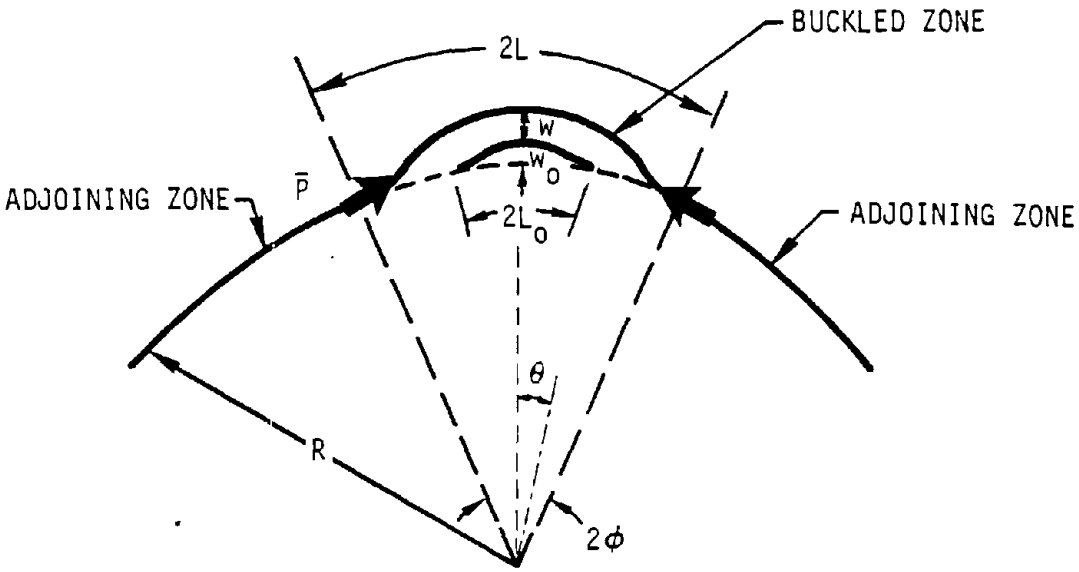

FIGURE 1. COORDINATE DEFINITION FOR CURVED TRACK

Boundary and Continuity Conditions

For the radial displacement w, we impose the following conditions:

At $\theta = 0$

$$\dot{w} \quad \text{(slope)} = 0 \tag{4.1}$$

$$\ddot{w} \quad \text{(shear force)} = 0 \tag{4.2}$$

At $\theta = \phi$

$$w = 0 \tag{4.3}$$

$$\dot{w} = 0 \tag{4.4}$$

$$\ddot{w} = 0 \tag{4.5}$$

In regard to the longitudinal displacements, we impose the following conditions:

At infinity

$$u = \dot{u} \rightarrow 0 \tag{4.6}$$

At $\theta = \phi$

$$u = U \tag{4.7}$$

$$\dot{u} = \dot{U} \tag{4.8}$$

At $\theta = 0$

$$U = 0 \tag{4.9}$$

Using the foregoing equations, it can be shown that

$$\alpha T = \frac{\bar{P}}{EA} + \frac{Z\psi}{(1 + \psi L)}$$

here

$$Z = \frac{1}{R} \int_0^{\phi} \left(\frac{\dot{w}^2}{2} + \dot{w}\dot{w}_o \right) d\phi$$

$$\psi = \sqrt{\frac{k_f}{EA}}$$

After determining the solution of the differential equation (1), the relationship between T and the maximum deflection w_{max} can be obtained. This determines the equilibrium response from which the buckling and the safe

temperature increase values can be determined. (In Figure 10, for example, T_B is the upper buckling temperature and T_S is the lower buckling temperature.)

Solution of the differential equation (1) is obtained using the Fourier approach, as described in Reference (4). The equation is nonlinear due to the nonlinear resistance F(w). This resistance was measured in the tests, as described in Section 3. In the case of vehicle loads acting on CWR, the loss of resistance due to "uplift" is computed as described in References (3,4).

3. TEST PARAMETERS AND MEASUREMENTS

3.1 TEST PARAMETERS

The major track characterization parameters measured during test conduct will be described in the following paragraphs.

Lateral Resistance

The resistance was measured using the Single Tie Push Test device (STPT) at a number of locations in the test zone, shown in Figure 2. The tests 1 and 2 in this figure refer to the static and the dynamic buckling tests, respectively. Although the initial resistance at the center location, 6, was high, it was subsequently reduced by pulling the track out for the purpose of setting the desired level of lateral misalignment. This reduced resistance is shown as 1,350 lbs. in Figure 2, and is used in the analysis of the static buckling test.

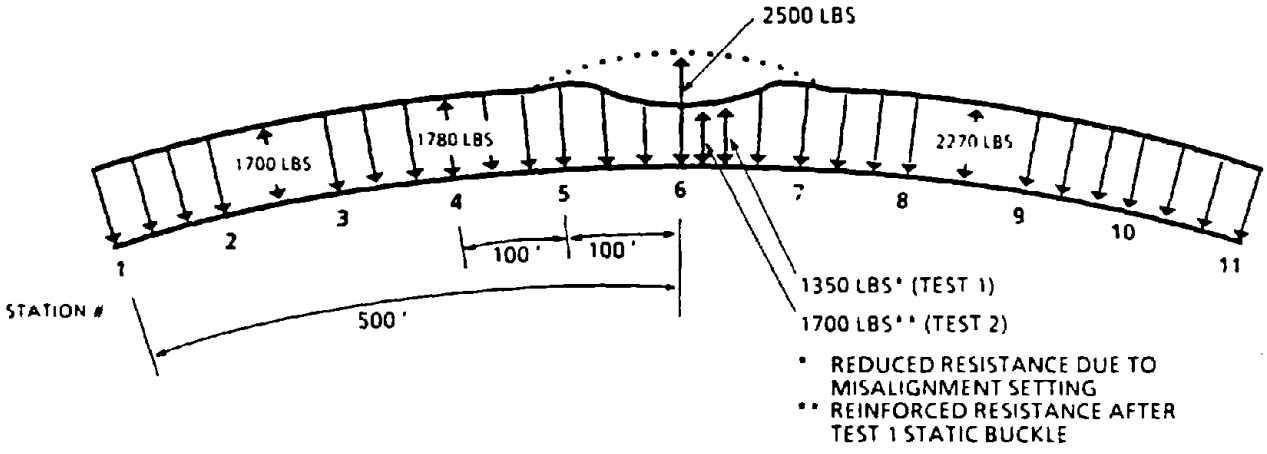

FIGURE 2. LATERAL RESISTANCE VARIATION IN TEST ZONE

The resistance at the location 4, determined by averaging the resistance values for six ties in the vicinity, is shown in Figure 3. The resistance has a typical softening behavior, observed in other tests. The resistance is idealized by the function, as shown in (5)

$$F(w) = F_p[k + (1 - k)e^{-\mu w}]$$

where

$k = F_p/F_L$ (peak to limiting value ratio)
μ = constant

This idealization is found to be convenient in the Fourier technique as it has a single functional form. Other idealizations such as the bilinear are not well suited for use in this technique.

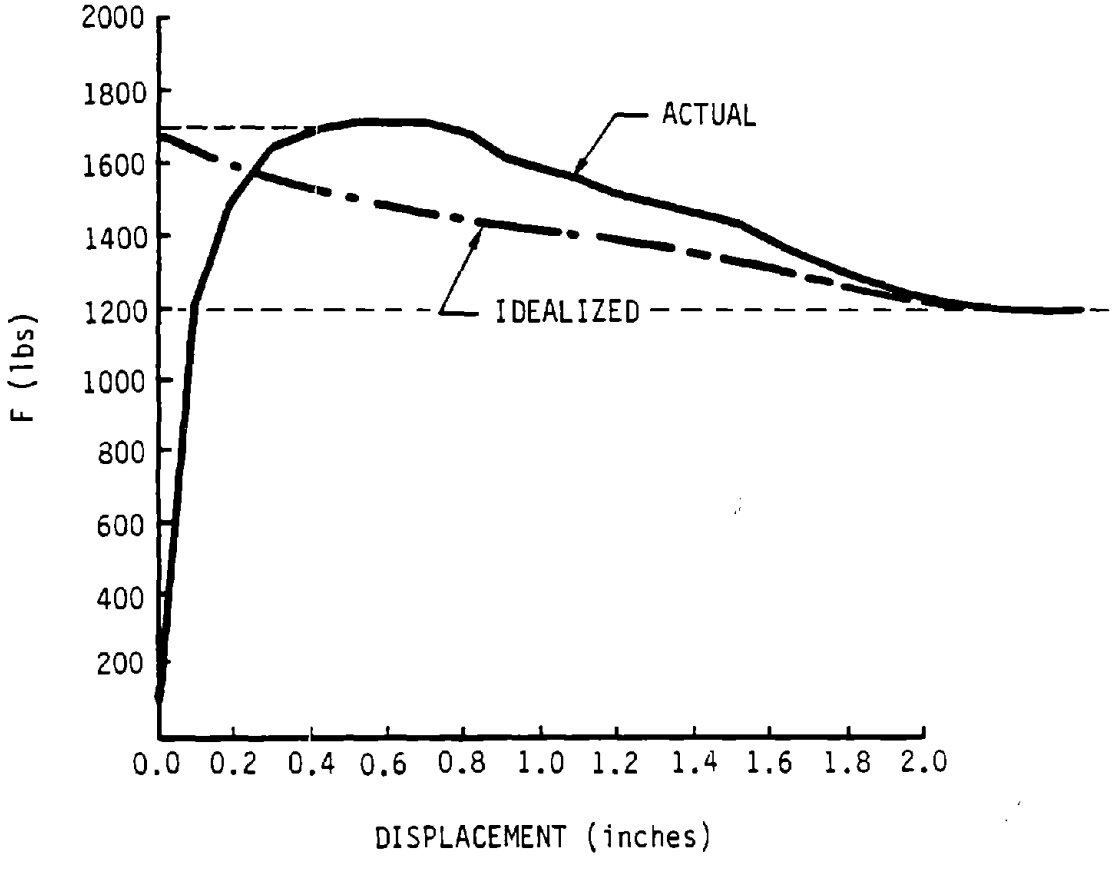

FIGURE 3. LATERAL RESISTANCE AT LOCATION 4

Lateral Misalignments

The lateral misalignments were mapped using the EM-80 track geometry car. The results are schematically shown in Figures 4 and 5 for the two tests. The misalignment at location 6 in test 1 was set intentionally at 1.5-in. amplitude to simulate to FRA Class 4 line defects. No attempt was made to alter other misalignments found prior to test 2, as these were considered to be representative of revenue service track line defects.

Other parameters required in the analysis are the longitudinal resistance and the vertical track modulus which were determined to be 200 lb/in./in. and 3,000 psi, respectively. The tie ballast friction coefficient which is also required in the analysis is assumed to be 0.7.

3.2 TEST MEASUREMENTS

The following measurements were recorded using the data logger during the test conduct:

a. Rail temperature using Resistance Temperature Detector (RTD) welded to the rail web ;

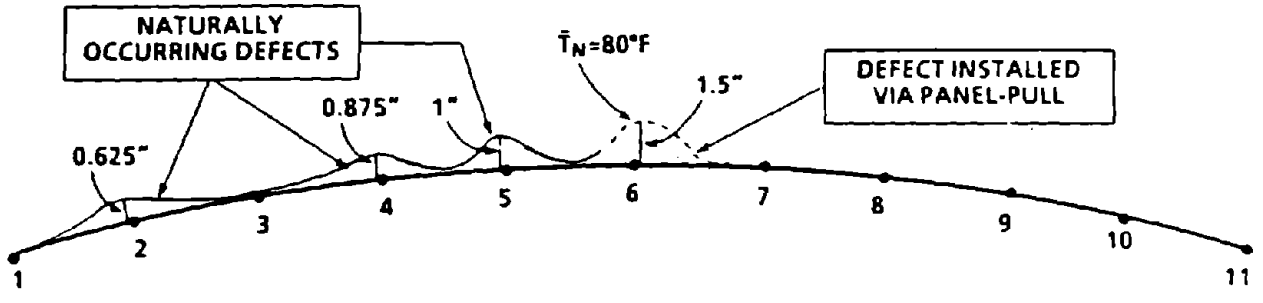

FIGURE 4. EM-80 TRACK GEOMETRY CAR LINE DEFECT MEASUREMENT - TEST 1

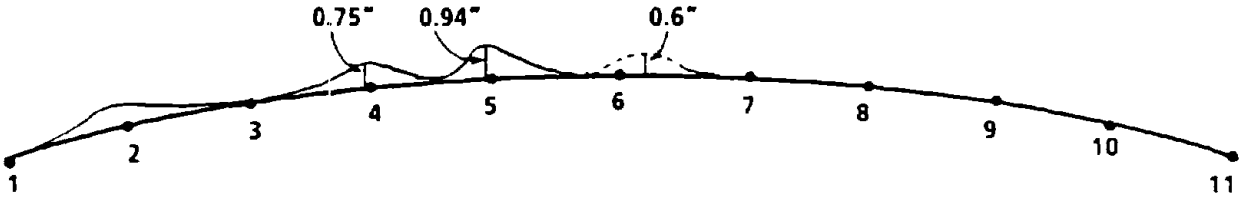

FIGURE 5. EM-80 TRACK GEOMETRY CAR LINE DEFECT MEASUREMENT - TEST 2

b. Longitudinal rail force using the standard four-arm strain gauge bridge. The rails were cut and destressed to provide a zero force reference for the strain gauges;

c. Lateral displacement of rails at several locations using rotary potentiometers;

d. Longitudinal displacements of rails at the ends, using rotary potentiometers;

e. Vertical loads on the rails due to vehicles using a strain gauge bridge ; and

f. Lateral loads generated on the rail, as the wheels negotiated the lateral imperfection, using a strain gauge bridge.

The instrumentation deployment is shown in Figure 6.

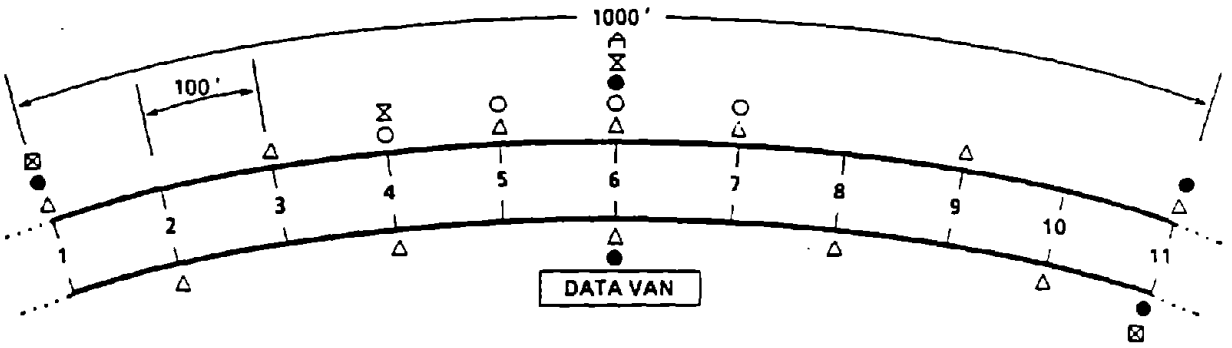

TEST ZONE (WOOD TIES)

····· STIFFENED ZONE *

1,2,....,11 STATION NUMBERS

△ LONGITUDINAL RAIL FORCE GAUGE (SG)

⧖ LATERAL FORCE GAUGE

⏢ VERTICAL FORCE GAUGE

● TEMPERATURE DETECTOR

○ LATERAL RAIL DEFLECTION TRANSDUCER

⊠ LONGITUDINAL RAIL DISPLACEMENT TRANSDUCER

* EVERY TIE ANCHORED, AND COMPRESSION CLIPS APPLIED

FIGURE 6. TEST ZONE INSTRUMENTATION

4. TEST CONDUCT

Rail Heating

The thermal force in the rails was artificially induced by electric heating. The current was drawn from internal circuits of two modified diesel locomotives. The modification involved disconnecting the traction motors and connecting the alternators to the rails. The heating locomotives were stationed on a siding at one end of the test zone.

Static Buckling Test (No. 1)

After setting a 1.5 in. amplitude imperfection at location 6, the rail heating was applied steadily until an explosive buckle occurred (Figure 7). The resulting buckling deflection was 13.5 in. The force distribution in the rails before and after buckling is shown in Figure 9(a). The buckle produced substantial reduction in the axial loads at locations 6 and 5.

Post Static Buckle Track Restoration

The overnight cooling of the rails pulled back the buckled track to 2-1/2-in. misalignment. The rails were cut at the

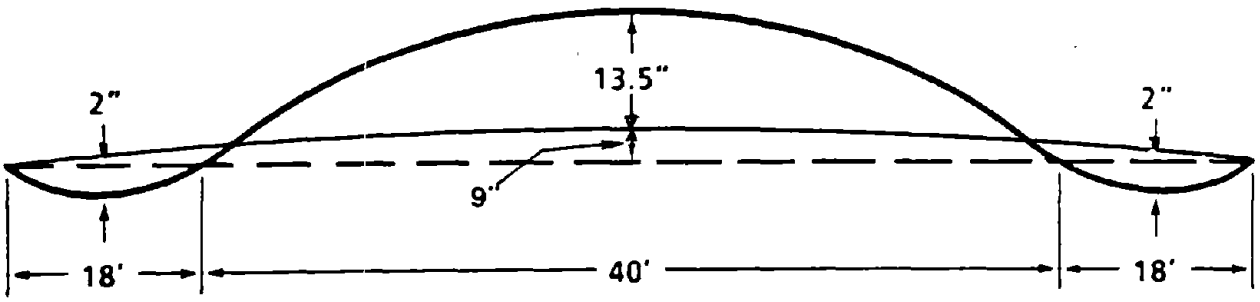

FIGURE 7. BUCKLED SHAPE OF RAILS (STATIC TEST)

center and after removing 1 in. from each rail, they were rewelded. For a 50 ft. segment in the central zone, additional ballast was dumped to strengthen the track locally. Additional strengthening was accomplished by placing concrete ties on the ends of the wood ties in this zone. The track was also anchored laterally to a "front-end loader." (See Appendix A, Photo Illustration.)

Dynamic Buckling Test (No. 2)

The misalignments were measured using the EM-80 car and locations 4 and 5 (see Figure 8) were identified to be buckling-prone. Lateral displacement transducers were installed at these locations to monitor the track movements during heating and vehicle traffic.

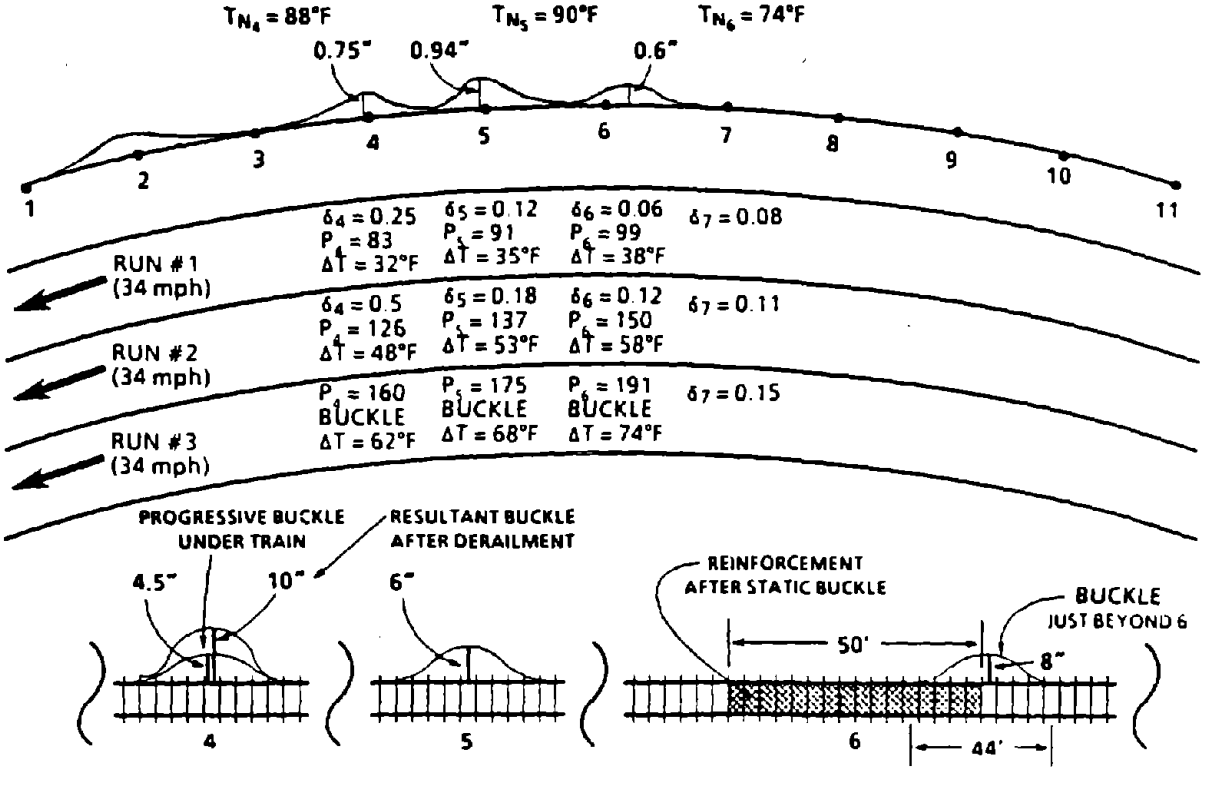

FIGURE 8. DYNAMIC BUCKLING TEST SUMMARY

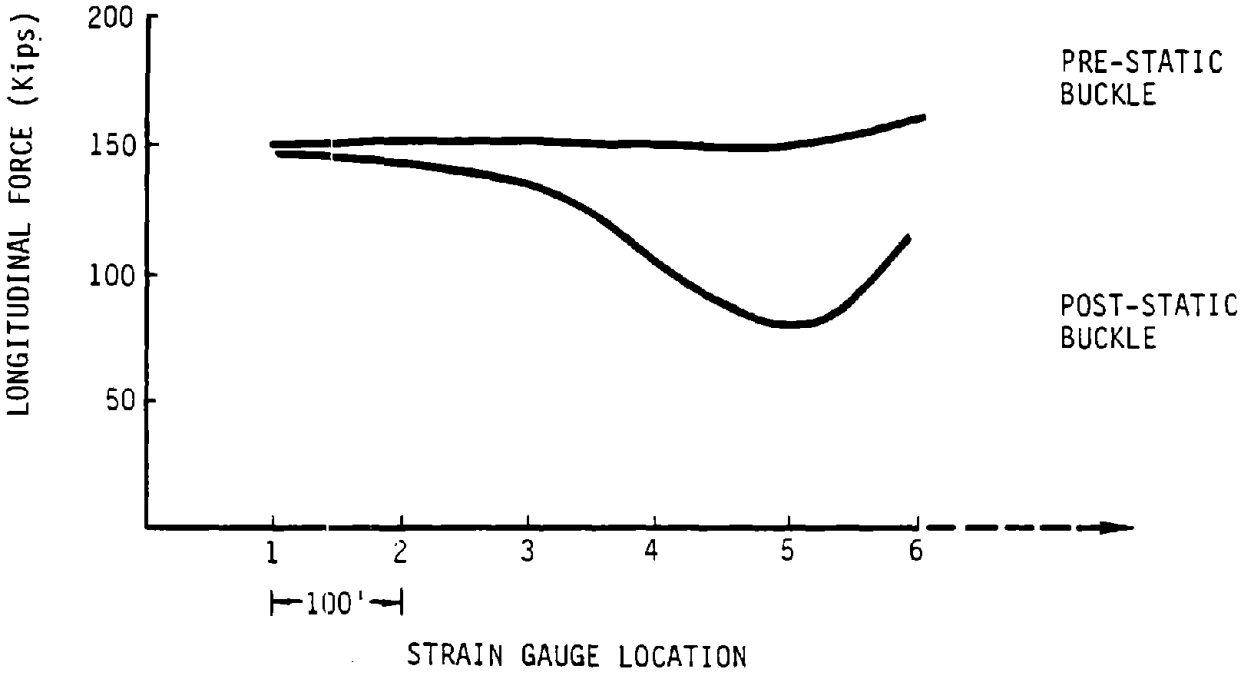

a) STATIC BUCKLING TEST

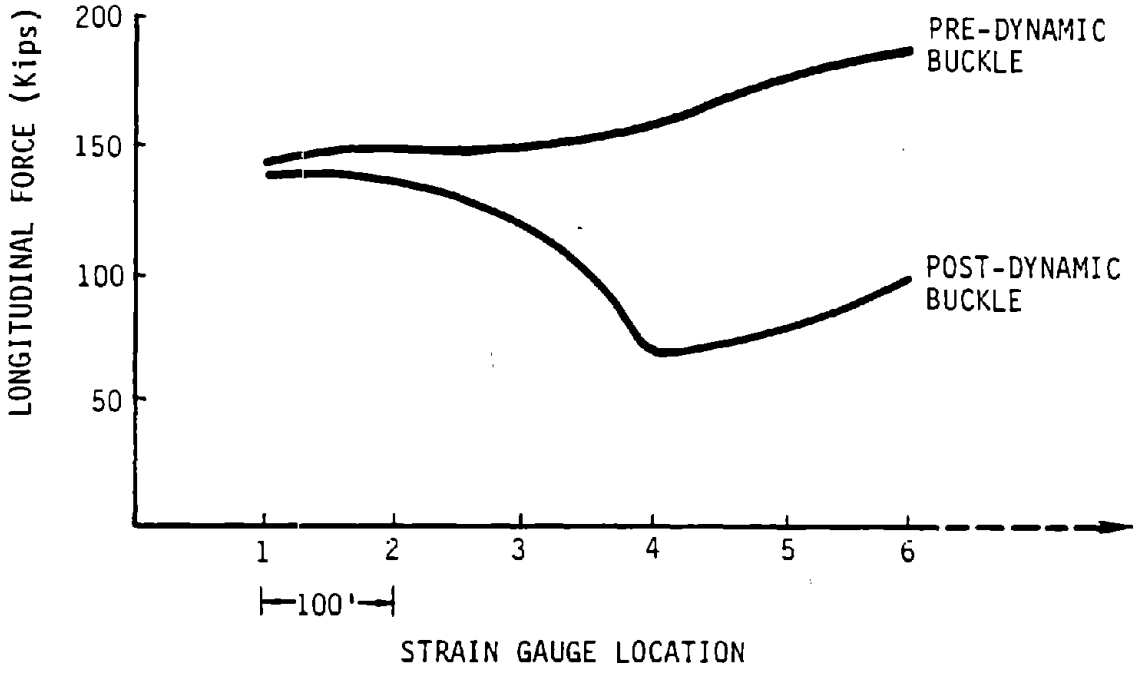

(b) DYNAMIC BUCKLING TEST

FIGURE 9. RAIL FORCE DISTRIBUTION

The consist used in this test had one empty and 23 loaded hopper cars and one GP-40 locomotive. Three runs at 34 mph (maximum allowable speed for the curve) were made at different rail temperatures.

The first run at a force level of 83 kips in each rail (at location 4) produced a misalignment increment of 0.25 in. over the initial value of 0.75 in. The second run at a rail force of 126 kips increased the deflection by an additional 0.25 in. The third and final run at 160 kips produced a buckle at all three locations (4, 5, and 6, see Figure 8).

The distribution of rail force before and after buckle is shown in Figure 9(b). Substantial drops in the rail force can be seen at the locations 4 to 6. The location 4 had the largest percent reduction in the rail force. Both 4 and 6 were buckling critical; the former is of more practical interest due to its lower buckling strength when compared with that of 6.

5. ANALYSES OF TEST RESULTS

Static Buckle

The theoretical and test results for the static buckle that occurred at the central location 6 are shown in Figure 10. The experimental buckling temperature increase of 66°F is close to the theoretical value of 69°F. The post buckled theoretical deflection of 13.5 in. is also in good agreement with the test result. However, the initial prebuckling displacement of about 1 in. observed in the test could not be predicted by the theory, since the theory neglects the initial linear part of the track resistance.

Dynamic Buckle

The theoretical results for run no. 3 and test results for the lateral deflection at location 4 are shown in Figure 11. The deflection growth was "stable" for run nos. 1 and 2 at 0.25 and 0.5 in., respectively, whereas for run no. 3, the deflection was continuously increasing due to the passage of the cars till a derailment occurred. The rail temperature in run no. 3 was 62°F whereas the "safe temperature" increase is 52°F according to the theory (Figure 11). Hence, the misalignment in run no. 3 was not stable, whereas in run nos. 1 and 2, the growth was limited because the rail temperatures were lower than the safe temperature. Figure 12 illustrates the contribution of individual cars to the growth of the lateral misalignment.

During run no. 3, buckles also occurred at locations 5 and 6. These were not analyzed in detail due to lack of data on the lateral resistance at these locations. Unlike at location 4, no significant growth of misalignment occurred at these locations prior to buckling. Hence, these buckles are considered to be explosive. The buckling force at location 6 was about 191 kips/rail and was 31 kips higher than the value

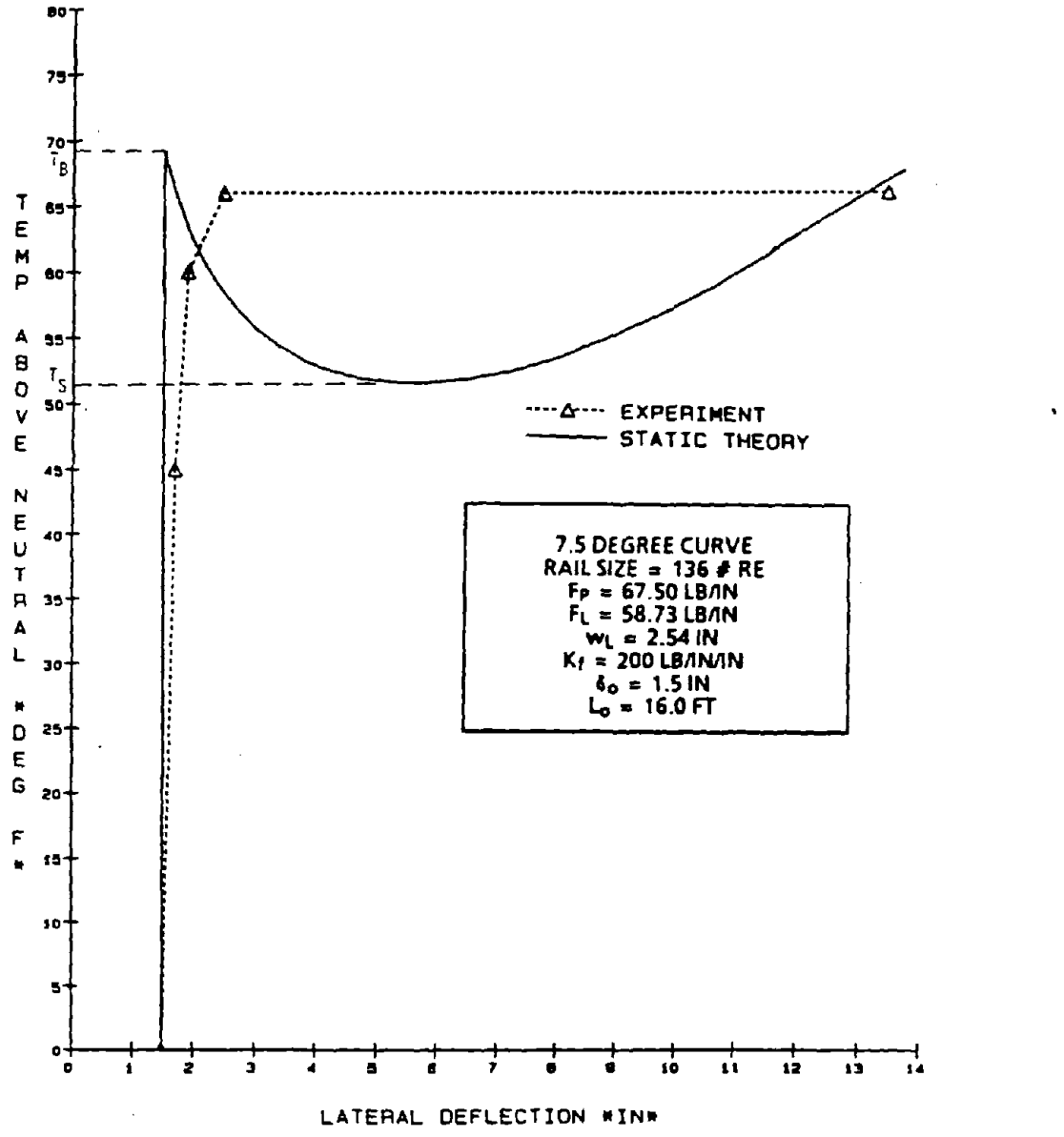

FIGURE 10. STATIC BUCKLE ANALYSIS VERSUS EXPERIMENT

at location 4. Explosive buckle is atypical for high degree weak curves and in this test, it could have been precipitated due to the increased strength at location 6 from the stiffening system used.

Portions of strip chart records of lateral displacement and force are presented in Figure 13(a,b), respectively. The progressive growth in the lateral displacement at location 4

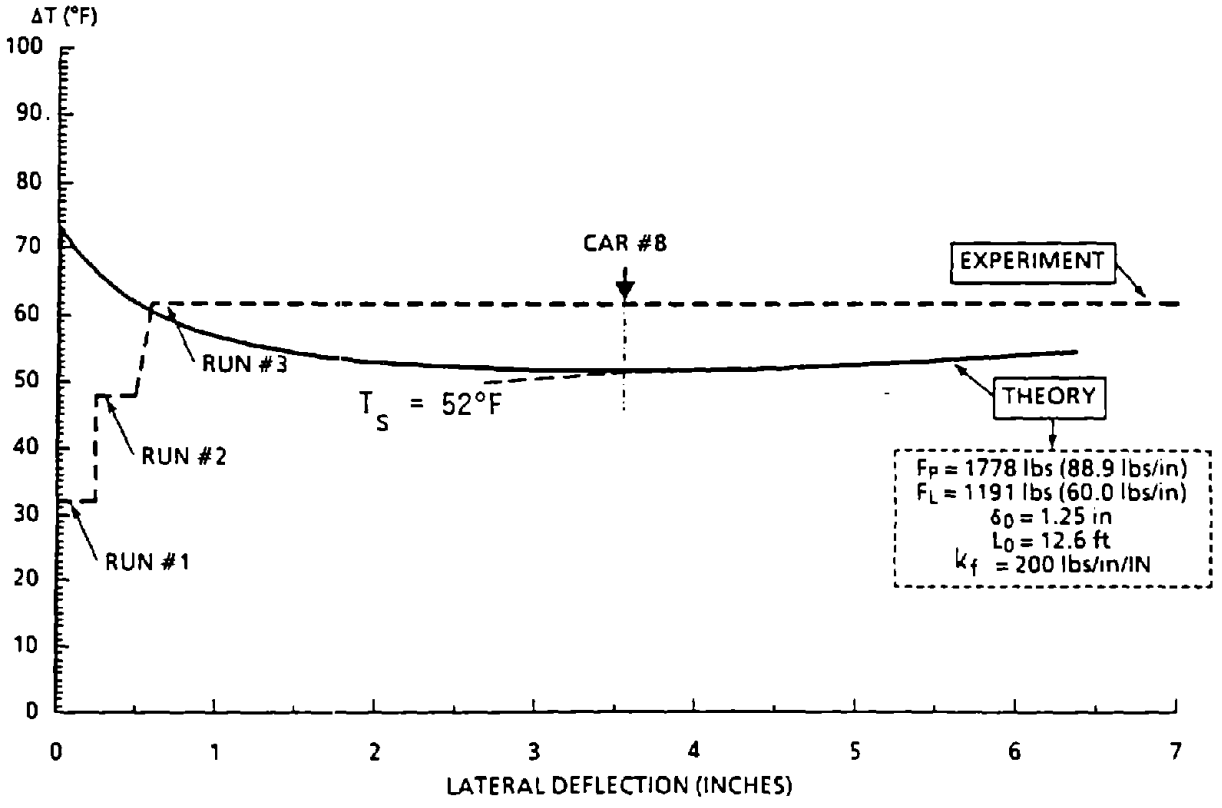

FIGURE 11. ANALYTIC VERSUS EXPERIMENTAL BEHAVIOR AT LOCATION 4

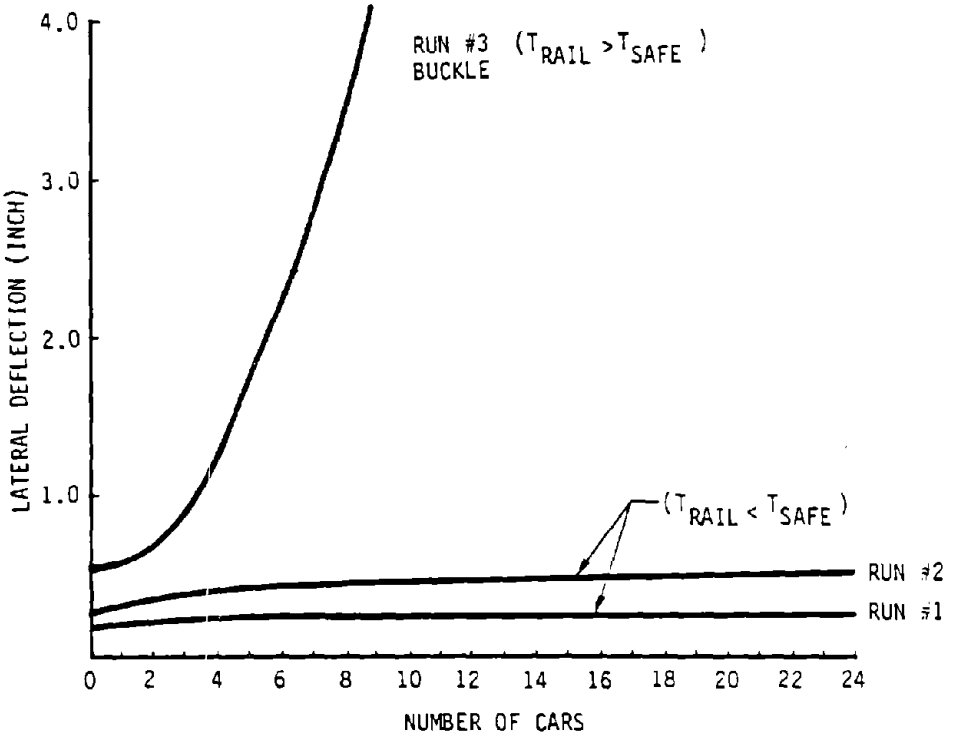

FIGURE 12. GROWTH OF LATERAL MISALIGNMENT UNDER CONSIST PASSES (LOCATION 4)

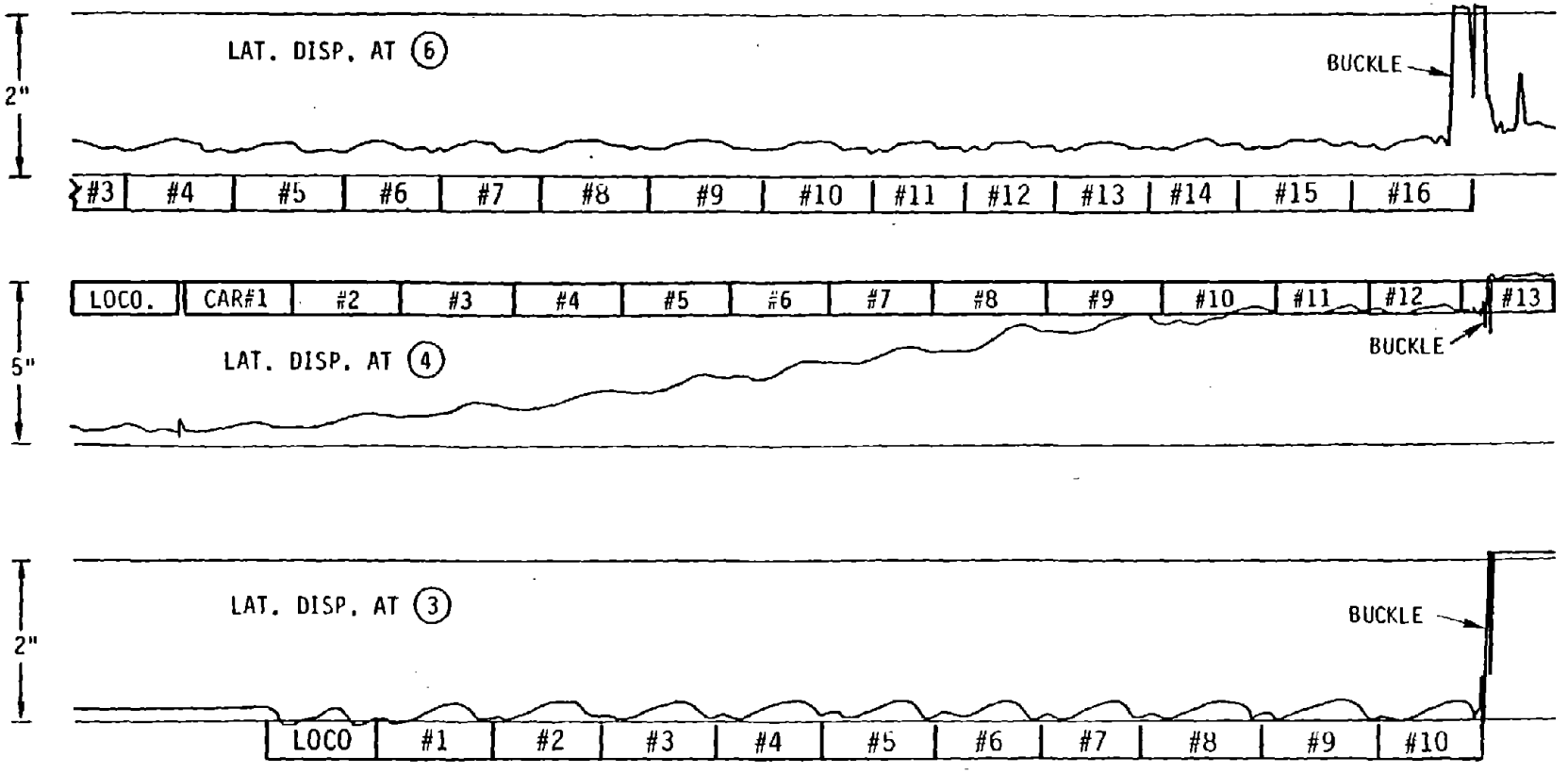

a) LATERAL DISPLACEMENT RECORD

FIGURE 13. STRIP CHART RECORD (RUN NO. 3)

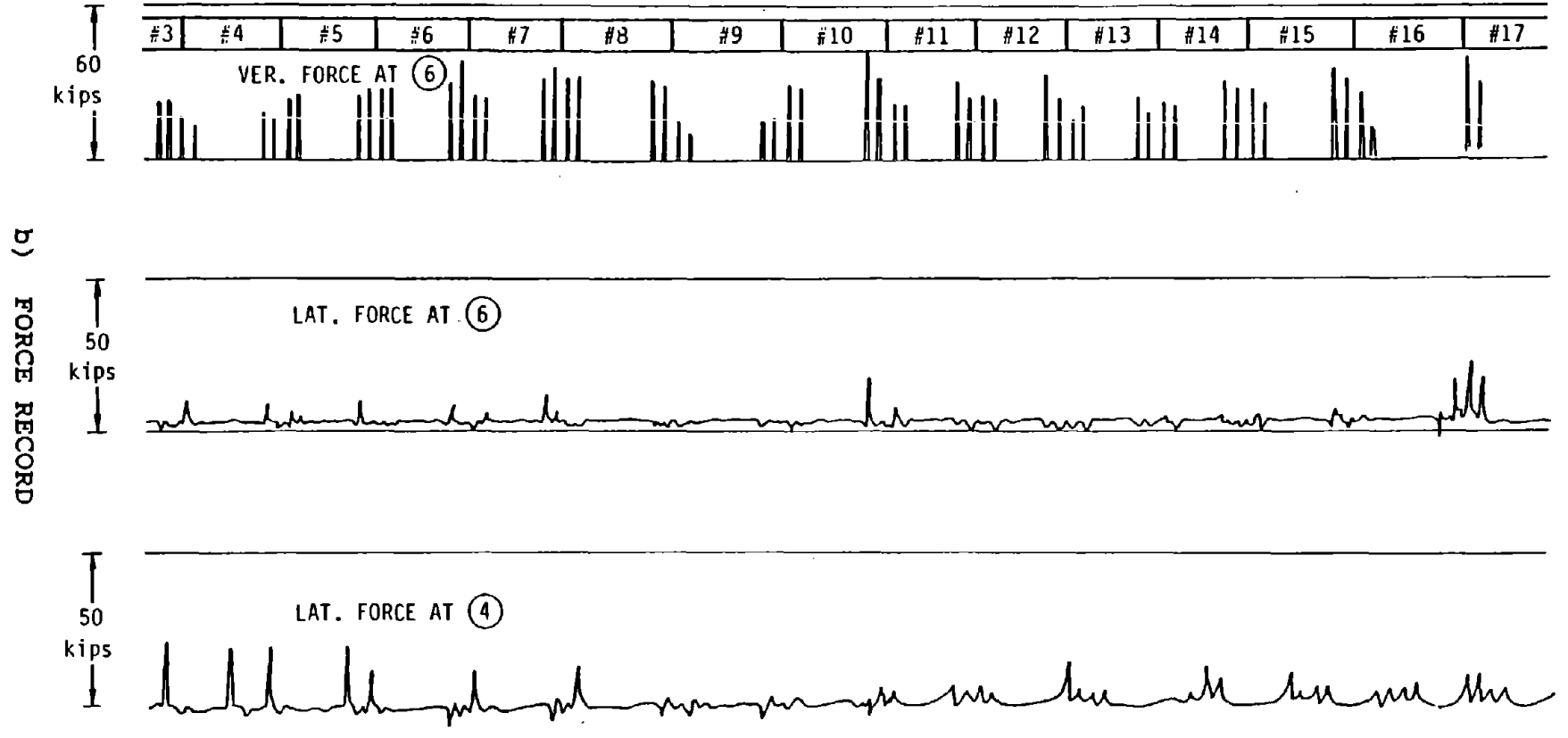

b) FORCE RECORD

FIGURE 13. STRIP CHART RECORD (RUN NO. 3) (CONT.)

can be seen in Figure 13(a). Also, the data indicate that the explosive buckle at 6 occurred first before the location 4 buckled to 10 in. from its value of 4.5-in. deflection. The progressive growth at the location 4 is typical for high degree curve. This growth was as critical as the explosive buckle at 6, particularly because this had occurred at lower rail force level. It is not known if the consist could have negotiated this progressive buckle, even in the absence of the explosive buckle at 6.

Derailment Analyses

The buckles during run no. 3 caused the derailment of six cars. Cars nos. 1 to 11 were ahead of the buckled locations. A buckle at location 6 occurred under car no. 12, but cars 12 to 15 negotiated the buckles exhibiting roll-type oscillations. Car nos. 16, 18, 21 to 24 derailed. The trailing trucks of cars 16 and 18 derailed at location 6. Derailed cars 16 and 18 could have contributed to the buckle at location 5. Car 21 trailing truck derailed at locations 5 and 4, whereas all the wheels of cars 22, 23, and 24 came off the rails.

The derailment of the trailing truck might indicate that the growth of misalignment occurred principally in-between the two trucks of the vehicle, which is in agreement with previous test data, thus showing the importance of central bending uplift wave in the dynamic buckling mechanism.

6. CONCLUSIONS

(i) For 7.5 degree CWR tracks with Class 4 type imperfections (1.5-in. line defect) and with resistance of 1,350 lb/tie the static buckling temperature is about 66°F. The dynamic buckling strength of this curve as measured by a 4.5 in. misalignment growth under the train with 1,780-lb/tie lateral resistance and with a line defect of 0.75 in. is less than 62°F. Such CWR tracks may be prone to buckle when carrying traffic on hot summer days when the rail temperature can reach 60°F over the neutral temperature.

(ii) When the rail temperature is above the lower dynamic buckling temperature, the train passes may produce rapid growth of lateral misalignment. For the 7.5 degree curve test, at the rail temperature of 10°F above the lower buckling temperature, each of the first eight cars passing over the misalignment increased the amplitude by about 0.5 in. Although the growth under the following cars could not be registered due to the transducer limitation, it may be inferred that for "stabilization" of the imperfection under vehicle passes, the allowable rail temperature should not greatly exceed the lower dynamic buckling temperature.

(iii) The growth of lateral misalignment takes place when the car center is over the imperfection, implying that the uplift bending wave in-between the trucks plays an important role in reducing the track lateral resistance and causing misalignment growth. The same conclusion has been reached in the earlier tests on tangent and the 5-degree curve (2). The presence of wheel-induced lateral forces would also influence the misalignment growth rate.

(iv) Buckling-induced derailment seems to occur at the trailing trucks. Known as the "third axle derailment," this

could be a principal cause of buckling-induced derailment in the revenue service CWR tracks.

(v) The static theory (absence of vehicle loads) gives reasonable predictions of CWR buckling behavior. The present buckling theory (4) predicts the lower buckling temperature satisfactorily, but slightly overestimates the ultimate dynamic buckling strength of CWR tracks. The factors contributing to the theoretical overestimates are possibly the quasi-static idealization of vehicle loads and the idealized lateral resistance that assumes a steep rise to its peak value.

6.1 Recommendations

(i) The issue of whether the track progressive lateral movement of 4.5 in. that occurred during the final test run is critical or not must be resolved. In the test, the effect of this progressive movement was overshadowed by the explosive buckle at the location 6. This location had a much higher level of force at the instant of buckling than the location at which progressive growth occurred. The issue should be resolved in a future buckling test.

(ii) If the allowable rail temperature is to be higher than the theoretical lower buckling temeprature of CWR to provide additional flexibility to the industry, a rational basis such as the energy criterion must be developed to assure safety of CWR against buckling. The present theory can be extended to provide the energy criterion.

APPENDIX A
PHOTO ILLUSTRATIONS

(Supplied by AAR/TTC Photo staff.)

FIGURE A-1. CONVERTED LOCOMOTIVES AND RAIL HEATING CONTROL SETUP

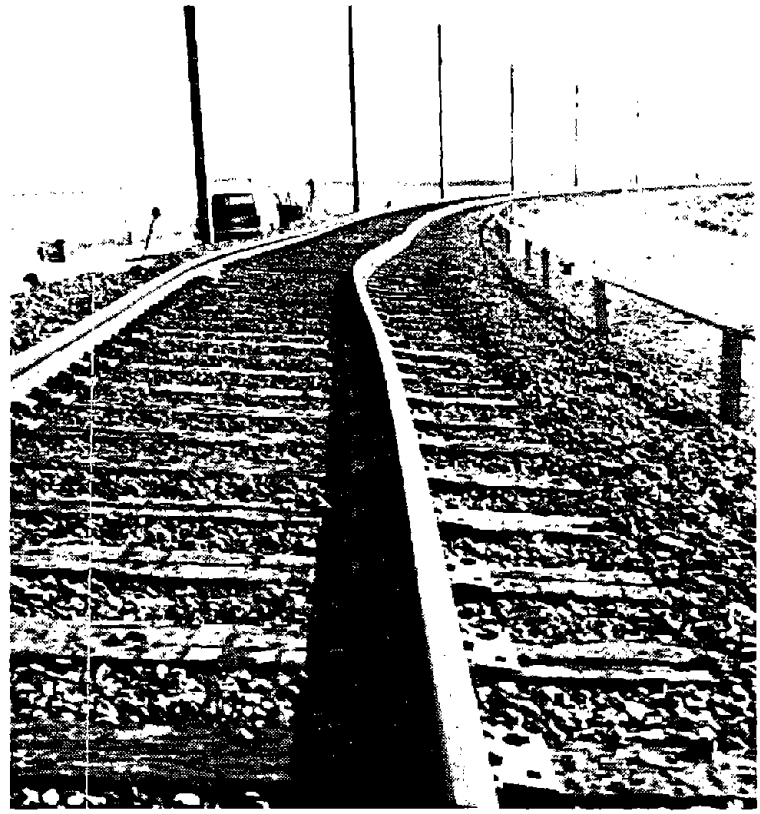

FIGURE A-2. STATIC BUCKLE AT LOCATION 6

FIGURE A-3. BALLAST ADDITION TO REINFORCE TRACK BUCKLED IN STATIC TEST

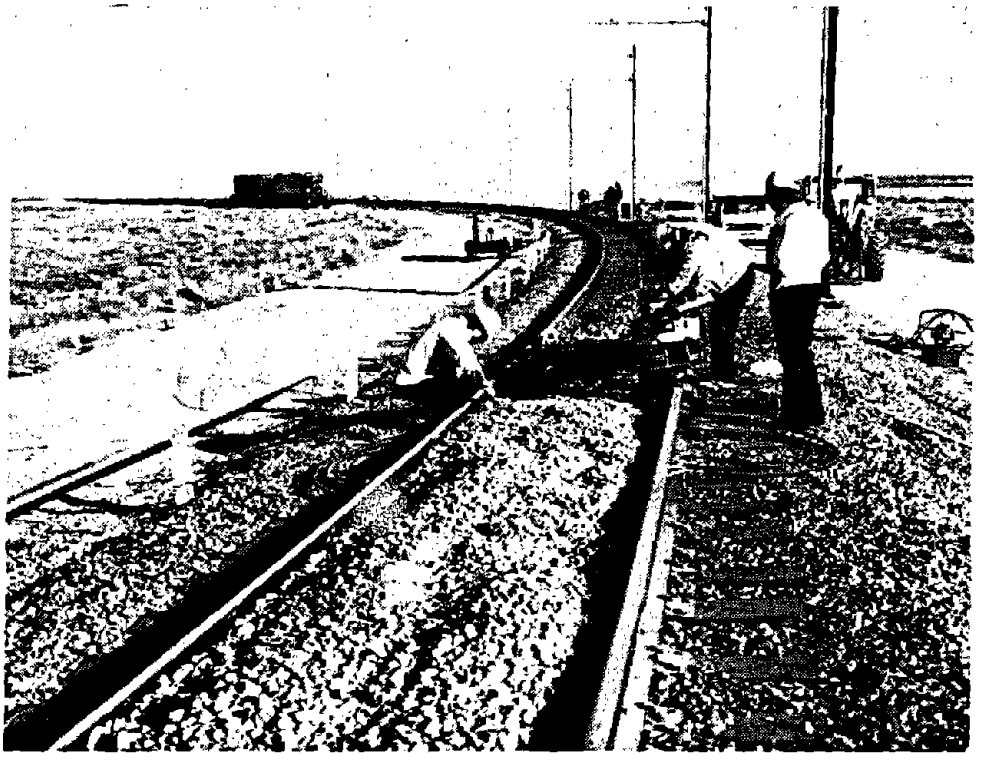

FIGURE A-4. STPT MEASUREMENT OF REINFORCED TRACK RESISTANCE

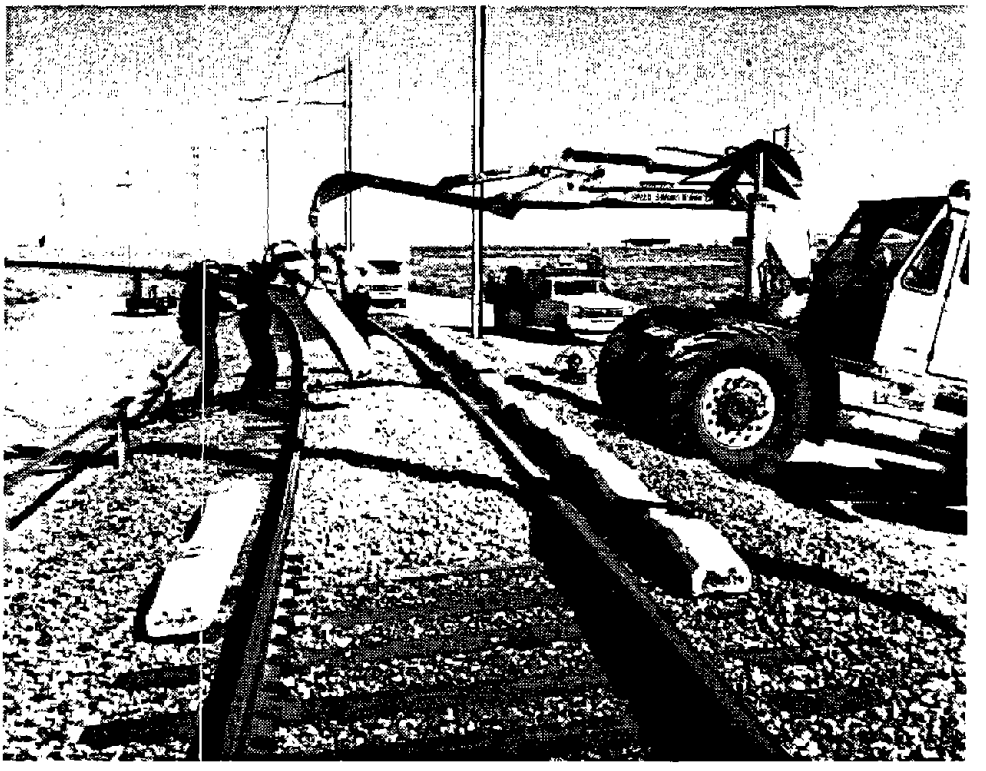

FIGURE A-5. ADDITIONAL STIFFENING FOR THE STATIC BUCKLED ZONE (CONCRETE TIES PLACED AT ENDS TO INCREASE WOOD TIE-BALLAST FRICTION)

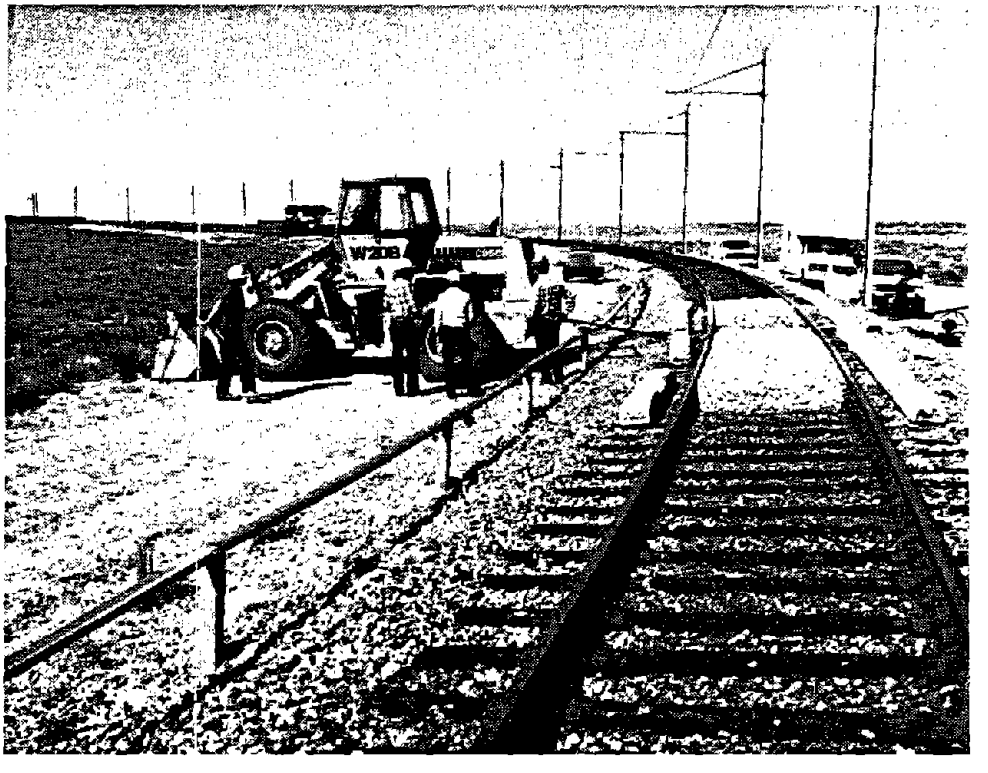

FIGURE A-6. FRONT END LOADER ANCHORED TO THE RAILS AT LOCATION 6

FIGURE A-7. TRACK CONDITION AFTER DERAILMENT

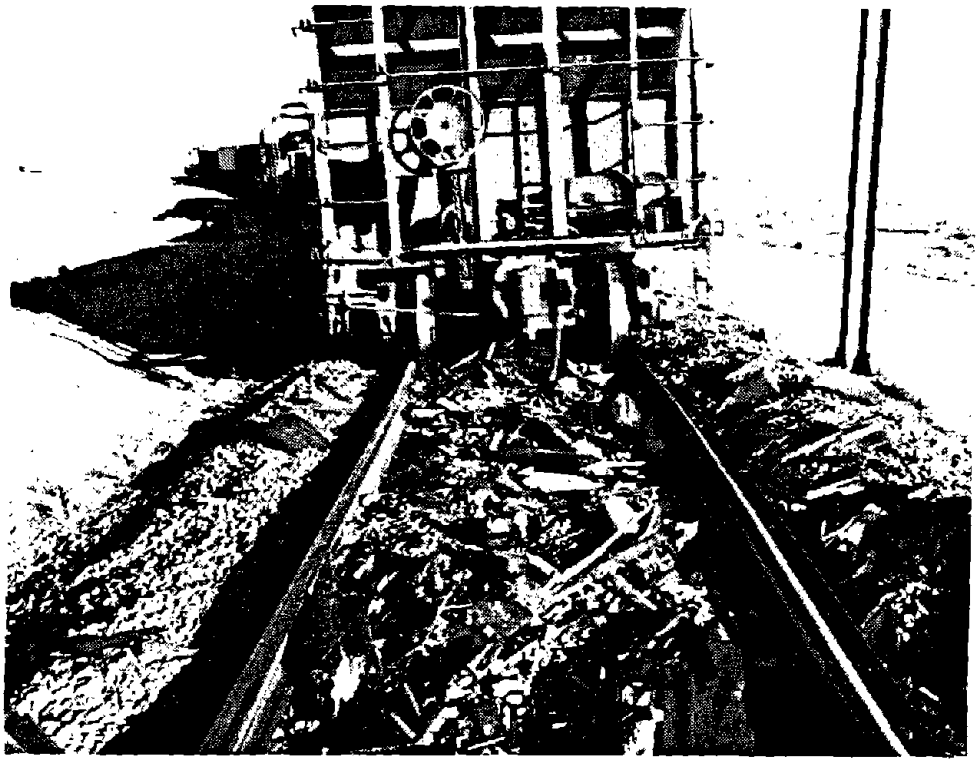

FIGURE A-8. LAST CAR DERAILED

FIGURE A-9. DYNAMIC BUCKLE NEAR LOCATION 6

FIGURE A-10. POST DERAILMENT VIEW AT LOCATIONS 4 AND 5

REFERENCES

1. Samavedam, G., A. Kish, and D. Jeong, "Experimental Investigations of Dynamic Buckling of CWR Tracks," DOT/FRA/ORD-86/07 (November 1986).

2. Samavedam, G., A. Kish, "Analyses of Phase III Dynamic Buckling Tests," DOT/FRA/ORD Report to be published.

3. Samavedam, G., "Buckling and Post Buckling Analyses of CWR in the Lateral Plane," Technical Note TN-TS-34, British Railways Board, R&D Division (January 1979).

4. Kish, A., G. Samavedam, and D. Jeong, "Influence of Vehicle Induced Loads on the Lateral Stability of CWR Track," FRA/ORD-85-3 (March 1985).

5. Samavedam, G., A. Kish, M. Thurston, and D. Jeong, "Recent Advances in Track Buckling Mechanics," ASME, AMD, Vol. 96, 1988.